ORIGINAL RESEARCH ARTICLE

M2 muscarinic receptor activation inhibits cell proliferation and migration of rat adipose-mesenchymal stem cells[†]

Running title: M2 receptor activation effects on ADSCs

Roberta Piovesana [1,2], Simona Melfi [2], Mario Fiore [3], Valerio Magnaghi [2§], Ada Maria Tata [1,4*]

[1]Department of Biology and Biotechnologies "C. Darwin", "Sapienza" University of Rome, Italy;

[2]Department of Pharmacological and Biomolecular Sciences, University of Milan, Italy;

[3]IBPM, Institute of Molecular Biology and Pathology, CNR, Rome, Italy;

[4]Center of Neurobiology "Daniel Bovet", "Sapienza" University of Rome, Italy

*Corresponding author**:** Prof. Ada Maria Tata, Dept. of Biology and Biotechnologies Charles Darwin, Sapienza, University of Rome, Italy, adamaria.tata@uniroma1.it; Tel. +39-06-49912822; Fax 39-06-49912351

§ Co-corresponding author: Prof. Valerio Magnaghi, Dept. of Pharmacological and Biomolecular Sciences, University of Milan, Italy, valerio.magnaghi@unimi.it; Tel. +39-02-50318413

[†]This article has been accepted for publication and undergone full peer review but has not been through the copyediting, typesetting, pagination and proofreading process, which may lead to differences between this version and the Version of Record. Please cite this article as doi: [10.1002/jcp.26350]

Received 13 August 2017; Revised 29 November 2017; Accepted 29 November 2017
Journal of Cellular Physiology

DOI 10.1002/jcp.26350

Abstract

Mesenchymal stem cells (MSCs), also known as stromal mesenchymal stem cells, are multipotent cells, which can be found in many tissues and organs as bone marrow, adipose tissue and other tissues. In particular MSCs derived from Adipose tissue (ADSCs) are the most frequently used in regenerative medicine because they are easy to source, rapidly expandable in culture and excellent differentiation potential into adipocytes, chondrocytes and other cell types.
Acetylcholine (ACh), is one of the most important neurotransmitter in central (CNS) and peripheral nervous system (PNS), playing important roles also in non-neural tissue, but its functions in MSCs are still not investigated. Although MSCs express muscarinic receptor subtypes, their role is completely unknown.
In present work muscarinic cholinergic effects were characterized in rat ADSCs. Analysis by RT-PCR demonstrates that ADSCs express M1-M4 muscarinic receptor subtypes, whereas M2 is one of the most expressed subtype. For this reason, our attention was focused on M2 subtype. By using the selective M2 agonist Arecaidine Propargyl Ester (APE) we performed cell proliferation and migration assays demonstrating that APE causes cell growth and migration inhibition without affecting cell survival. Our results indicate that ACh via M2 receptors, may contribute to the maintaining of the ADSCs quiescent status. These data are the first evidence that ACh via muscarinic receptors might contribute to control ADSCs physiology.

Keywords: Muscarinic receptors; acetylcholine; adipose derived stem cells; proliferation; migration.

Introduction

All tissues have hierarchical cellular organization; these include a small number of stem cells and differently derived cell types. Stem cells are immature precursor cells, unspecialized, with ability to perpetuate themselves (self-renewal), maintaining the same undifferentiated stage and the potential to generate mature cells through asymmetric division. Through this process, stem cells generate one stem and one daughter cell, with specific fate. Stem cells are quiescent cells (in G0 phase) or characterised by a slow proliferation rate and normally they are maintained in an undifferentiated state until they are required to support physiological cell turnover. Stem cells are also able to divide through symmetrical division, leading to the formation of two daughter cells with identical self-renewal capacity, maintaining the stem cell pool. Thereby, stem cells can differentiate in specialised cells (Weissman, 2000). The asymmetric division allows to control the stem cell number in the tissue, which may remain constant at least during the adult life. Notably, the low replication rate reduces the probability to accumulate DNA damage and mutations (Ilic et al, 2011).

There are various types of stem cells, whose identity is determined by their origin and differentiative potential, such as totipotent cells, pluripotent cells, unipotent stem cells. Mesenchymal stromal cells (MSCs) derived from the mesoderm, the middle germ layer that during embryogenesis originates different tissues and cells, such as connective, condrocytes, bone, endotelial and muscle cells. MSCs can also interact with hematopoietic stem cells (HSCs), giving rise to immunomodulatory mechanisms (Chamberlain et al, 2007). Bone marrow stem cells have been widely proposed and used in regenerative medicine as source of MSCs (Caddick et al, 2006). Giving their high invasive procedure of collection, in the last decade some criticisms were raised about their use. For instance, it has been observed low cell proliferation with slow *ex vivo* expansion and incresed senescence, directly correlated to the age of the donor (Caddick et al, 2006). For these reasons, the identification of an alternative source of MSCs is required.

Adipose tissue is constituted by small blood vessels, nerve cells, fibroblasts, as well as by adipocyte progenitors, known as pre-adipocytes or adipose derived mesenchymal stem cells (ADSCs) (Vindigni et al, 2013). ADSCs can be easily isolated by conventional liposuction, a less invasive procedure compared to the bone marrow sampling (Kingham et al, 2007).

In vitro ADSCs share many characteristic features of Bone Marrow MSCs: stickiness to plastic, fibroblastoid morphology and potential differentiative capacity under appropriate conditions, into osteoblasts, adipocytes and chondroblasts (Strem et al, 2005; Frith et al, 2008). MSCs can be easily isolated: they are positive for a lot of specific markers, such as the antigens CD105, CD73, CD44, CD29 and CD90. Contemporarily, MSCs are negative for the antigens CD45, CD34, CD14, CD11b, CD79a, CD19 and HLA-DR (Strem et al, 2005; Bobis et al, 2006).

ADSCs possess the typical stem cells ultrastructure, including the high nucleus/cytosol ratio, exhibit prominent nucleoli and numerous cytoplasmic organelles (Patel et al, 2013; Ryu et al, 2013).

In general, ADSCs are easy to source and present lack of immunogenicity, enabling allogenic transplantation without the use of immunosuppressive drugs. Moreover, the lack of ethical controversies make them of potential interest in tissue-specific differentiation (Grimble et al, 2007; Karp et al, 2009). ADSCs possess multi-differentiate properties and act as a "secretome", releasing proteins and growth factors in the extracellular matrix (ECM), with a high impact on the different organs and systems (Vindigni et al, 2013). For all these properties, ADSCs appear a good cell candidate in the field of regenerative medicine and gene therapy.

In recent years, the scientific community consolidated the concept of the presence of a non-neuronal cholinergic system, whose first demonstration has been described in the placenta (Morris, 1966). The cholinergic system is expressed in the skin, in the respiratory and immune system, where it is involved in the proliferation, differentiation and survival/apoptosis of different cell types (Skok et al, 2006; Hoogduijn et al, 2009). MSCs are regulated by a variety of intracellular and extracelluar signals such as BMPs, Notch, Wnt, IFNγ and many other signaling pathways not yet identified (Hoogduijn et al, 2009). The widespread expression of the

cholinergic system in non-neuronal tissues has suggested that the specific neurotransmitter acetylcholine (ACh) may have a role in the regulation of cell physiology in different cell types (Wessler et al, 1999). In this light, it has been recently shown that the nicotinic receptor stimulation in embryonic mouse stem cells regulates Oct-4 and Rex-1 markers (Zhang et al, 2015). In mammals, however, the cholinergic system achieves the full maturation after birth (Berger-Sweeney et al, 1997), suggesting that this system may play important role in adult stem cells. Moreover, more recent evidence reported the presence of ACh in different stem cell niches including hippocampal dentate gyrus subgranular zone (SGZ) and in lateral ventricular zone (LV) of the mammalian brain, suggesting that cholinergic signals may contribute to the modulation of adult neural stem cell physiology (Asrican et al, 2016). Interestingly, MSCs have also the ability to produce ACh, having a positive staining for ChAT (Hoogduijn et al, 2009). However, no clear evidence on the role of ACh in ADSCs has been described, nonetheless a full characterization of muscarinic and/or nicotinic receptor subtypes in ADSCs was performed (Hoogduijn et al, 2009).

In this study, using stem cells isolated from rat adipose tissue, the role of ACh and muscarinic receptors was investigated in ADSCs development and physiology. In detail, the muscarìnic receptor subtypes expressed has been characterized in ADSCs, focusing on the effects produced by the selective activation of M2 subtype, whose ability to modulate cell proliferation and differentiation has been previously described in different cell types (De Angelis et al, 2012; Uggenti et al, 2014; Alessandrini et al 2015). The results obtained demonstrate that ADSCs cell proliferation and migration are affected by M2 selective activation.

Material and Methods

Adipose derived stem cells

ADSCs were kindly provided by Professor Reid, University of Manchester, UK. However ADSCs were isolated from adult Sprague-Dawley rats as previously described (Kingham et al, 2007). Subcutaneous, visceral and inguinal fat pads were passed through a 100μm cell strainer after mechanical and enzymatic dissociation with collagenase type I (Life technologies, Monza, Italy). The resulting cell suspensions were pelleted by 5 min of centrifugation at 900 rpm, resuspended in α-MEM plus 10% (v/v) FBS (Sigma-Aldrich, St. Louis, MO, USA) and plated onto 75 cm^2 flasks. When confluent, cells were detached with trypsin-EDTA (Life Technologies, Monza, Italy). The cells were mantained in α-MEM (Sigma-Aldrich, St. Louis, MO, USA) containig 10% (v/v) FBS (Sigma-Aldrich, St. Louis, MO, USA) and 1% Penicillin/Streptomycin solution (Sigma-Aldrich, St. Louis, MO, USA). Cultures was mainteined at sub-confluent levels at 37°C in umidified atmosphere with 5%CO_2-95% air.

Cell treatments

The cells were treated with M2 muscarinic receptor agonist, Arecaidine Propargyl Ester hydrobromide (APE, Sigma-Aldrich, St. Louis, MO, USA) at the final concentration of 100μM. The APE selectivity for M2 receptors was largely confirmed by siRNA transfection for M2 receptors and by pharmacological binding experiments (Alessandrini et al, 2015). According previous experiments, muscarinic antagonists were used at the final concentration of 10^{-7}M for Methoctramine (M2 antagonist, Sigma-Aldrich, St. Louis, MO, USA), 10^{-7}M for Pirenzepine (M1 antagonist Sigma-Aldrich, St. Louis, MO, USA) and 10^{-8}M for 4-DAMP (M3 antagonist Sigma-Aldrich, St. Louis, MO, USA), (Ferretti et al, 2013, Alessandrini et al, 2015). The cells were treated with muscarinic receptor antagonist 2h before APE treatment.

RT-PCR analysis

Total RNA was extracted using Tri-Reagent (Sigma-Aldrich, St. Louis, MO, USA) and digested with DNAseI (Ambion-Life technologies Italia, Monza, Italy). Two µg of total RNA was reverse transcripted into cDNA with 1µg of random Primers (Promega, Madison, WI, USA) and 200U of Moloney Murine Leukemia Virus (M-MLV) reverse transcriptase (Promega Madison, WI, USA). Glyceraldehyde-3-phospate dehydrogenase (GAPDH) was used as the housekeeping gene. The sequences of the primers used in RT-PCR analysis are reported in Table 1.

Western Blot

Protein samples were extracted in Lysis buffer (10nM Tris, 0,5% NP40, 150mM NaCl). Sample buffer (4X) was added to the protein sample, heated for 5 minutes at 100°C and then loaded onto a 10% SDS polyacrylamide gel and run at 30mA using running buffer (25 mM Tris, 190 mM glycine, 0,08% (w/v) SDS). SDS-PAGE gels were transferred for 2h onto PVDF membranes (Millipore, Billerica, MA) at 200 mA in transfer buffer (20mM Tris; 150 mM glycine, 10% (v/v) methanol). After 5% non-fat dry milk block (Cell Signalling Technology, Davers MA, USA), the membranes were incubated overnight at 4°C, with the primary antibody, previously diluted in the blocking solution.The mouse anti-M2 primary antibody (1:500; Abcam, UK RRID:AB_303318), mouse anti-PCNA (1:700; Sigma-Aldrich, St. Louis, MO, USA, RRID:AB_1842895); rabbit anti-CXCR4 (1:300; Novusbio, UK; RRID:AB_10001320) and rabbit anti-CXCR7 (1:300; Abcam,UK; RRID:AB_880133) were used. Actin was used as protein reference (anti-actin, 1:6000, Millipore, Milan; RRID:AB_223041). Membranes were incubated with HPR-conjugated secondary antibody (1:20000, Promega, Madison, WI, USA). Protein expression was detected by using enhanced chemiluminescence (ECL) (Euroclone, Pero, MI, Italy).

Immunocytochemistry

ADSCs were plated onto 12 multiwells in complete medium (α-MEM containig 10% FBS and 1% Penicillin/Streptomycin solution) (Sigma-Aldrich, St. Louis, MO, USA). The following day, cells were treated as required by experimental plan. Then they were washed with PBS twice and fixed with 4% paraformaldehyde in PBS for 20 min at room temperature (RT). After three washes in PBS, the cells were pre-incubated in PBS solution containing 0.1% Triton X-100 and 10% normal goat serum (NGS) for 1 h at RT. Then cells were incubated with a monoclonal anti-M2 antibody (1:200, Abcam, UK, RRID:AB_303318) at 4 °C overnight. The next day, the cells were washed with PBS three times for 10 min. After washes, cells were incubated with goat anti-mouse IgG-Alexa 594 conjugated (Promega Italia, MI, Italy) (diluted 1:500 in PBS+ 0.1% Triton X-100 + 1% NGS) for 2 h at RT. After three washes in PBS, the slides were mounted with Vectashield (H1200, Vector Lab, DBA, Milan, Italy).

Migration assays

To evaluate cell migration, the wound healing and the Boyden chamber assays were used.

For wound healing assay the cells were plated on 60 mm^2 ∅ dishes and then treated with 100μM APE (Sigma-Aldrich, St. Louis, MO, USA) for 6h. Cells were treated with muscarinic receptor antagonist (Methoctramine 10^{-7}M, Pirenzepine 10^{-7}M and 4-DAMP 10^{-8}M) (Sigma-Aldrich, St. Louis, MO, USA), 2h before APE treatment. The scratch was made up with p200 tip, then the Mitomicin C (50ng/ml, Sigma-Aldrich, St. Louis, MO, USA) was added to the culture medium, to exclude a possible influence of cell proliferation. The cells were photographed at the start (t0) and after 6h (t6). The space between the two fronts at the start and after 6h was then measured. The two values were subtracted (t0-t6), obtaining the covered space by the cells in the experimental time chosen.

Migration was also tested by Boyden's assay, using a 48-well chamber, according to manufacturer's instructions (Neuroprobe, Cabin John, MD, USA). Cells were treated with

100µM APE, as described above. DMEM/1%FBS was placed in the lower compartment of the chamber, as chemo-attractant. The open-bottom wells of the upper compartment were filled with cells (10^5cells/well), collected by trypsin and suspended in DMEM + 0.1 % bovine serum albumin (BSA, Sigma). Cells migrate through a polyvinylpyrrolidone-free polycarbonate porous membrane (8µm pores) pre-coated with gelatine (0.2mg/ml in PBS, 5 days at 4°C). After migration (overnight, 37°C), cells adherent to the underside of the membrane, were fixed by methanol and stained according to the Diff-Quik kit (Biomap, Milan, Italy). For quantitative analysis, 3 random objective fields for each well were counted, using a 20x objective on an optical microscope; the mean number of migrating cells was calculated.

MTT assay

To evaluate the cell viability, ADSCs were seeded on 24-well plate at the density of 25×10^3cells/well. After 24h cells were treated with 100µM APE (Sigma-Aldrich, St. Louis, MO, USA) at 24, 48, and 72h. Cells were also treated with muscarinic receptor antagonist (10^{-7}M Methoctramine, 10^{-7}M Pirenzepine and 10^{-8}M 4-DAMP; Sigma-Aldrich, St. Louis, MO, USA) 2h before APE treatment. Cell growth was assessed by colorimetric assay based on 3-(4,5-dimethyl thiazol 2-y1)-2,5-diphenyl tetrazolium bromide (MTT, Sigma-Aldrich, St. Louis, MO, USA). For each well, the OD at 570 nm was measured by GloMax Multi Detection System (Promega, Madison, WI, USA).

Flow Cytometry analysis

The cells were plated on 60-mm diameter dishes at a density of $2x10^4$ cells/dish. The day after plating, the cells, excluding control samples, were treated with 100µM APE for 48, 72 and 96h. At the end of the treatment, cells were incubated for 90 min with 45µM bromodeoxyuridine (final concentration) (BrdU, Sigma-Aldrich), collected by trypsinization, centrifuged for 10min at 1,000 rpm and then fixed in methanol/PBS 1:1 (v/v). To identify cells in S phase, DNA content and BrdUrd incorporation were determined in simultaneous analysis by staining with

propidium iodide (PI) and anti-BrdU respectively. Partial DNA denaturation was performed by incubating the cells in 3N HCl for 45 min, followed by neutralization with 0.1 M sodium tetraborate.

Samples were then incubated with monoclonal anti-BrdU (1:50 v/v; Dako, Santa Clara, CA, USA; RRID:AB_10013660) for a further 30 min at RT, washed twice with 0.5% Tween-20 in PBS and incubated for 30 min with antimouse Alexa 488 fluor-conjugated (1:600) (Promega Italia, MI, Italy). Samples were washed twice with PBS plus 0.5% Tween-20 and finally stained with 10µg/ml PI for 15 min at RT. Flow cytometry analysis was performed with a flow cytometer Coulter Epics XL with 488 nm wavelength excitation and 10^4 events were collected for each sample. Biparametric (DNA content versus BrdU content) analysis were performed using WinMDI 2.7 software.

Recovery

To assess whether inhibition of cell proliferation-APE induced was reversible, a recovery analysis was set up. The cells were treated for 96h with APE. Then the medium containing APE was eliminated and the cells were washed with PBS and fresh complete medium without APE was added. Growth analysis was assessed by MTT assay (Sigma-Aldrich, St. Louis, MO, USA). For each well, the OD at 570nm was measured by GloMax Multi Detection System (Promega, Madison, WI, USA), at different time points after 96h of APE treatment (72-168h).

Cell viability assay

Cell viability was evalutated by trypan blue staining. Ten µl of trypan blue solution (1:10 *v/v*) (Sigma-Aldrich, St. Louis, MO, USA) was added to 90µl of cell suspension. After 5 min, the number of blue-stained cells (not viable) and unstained cells (viable) was evaluated using Bürcker chamber (data not shown). The cell viability was also analysed by LUNA cell Counter and the data were presented as percentage of live cells/total cells.

Data analysis

Data analysis were performed with GraphPad Prism (GraphPad Software Inc, La Jolla, CA, USA). Data was presented as the mean ± SEM. Student's *t* test or one-way ANOVA analysis with Bonferroni' or Tukey's post tests were used. A value of $p < 0.05$ was considered statistically significant: $p < 0.05$ (*), $p < 0.01$ (**) and $p < 0.001$ (***). The densitometric analysis of the RT-PCR and Western blot analysis was measured by ImageJ software (NIH, USA: RRID: SCR_003070).

Results

Expression of stemness markers and muscarinic receptors

ADSCs are positive for different markers including CD29, CD44, and CD90 (Bobis et al, 2006). To validate stemness property, the expression of these stemness markers were determined by RT-PCR analysis. The results were compared to fibroblasts, as differentiated cells (Fig.1A). These results demonstrated higher levels of stemness markers expression in ADSCs compared with differentiated fibroblast population, confirming the stem cell nature of our cultures. Then, the muscarinic receptor subtypes expression were characterised by semiquantitative RT-PCR analysis. As showed in Fig.1B the ADSCs express the transcripts for several muscarinic receptor subtypes (M1-M4), whereas the expression of M5 subtype resulted undetectable. The M2 and M3 subtypes appeared the most abundant muscarinic receptors in ADSCs. However, considering the well characterized role of M2 receptors in the control of cell proliferation and migration of other cell types (Loreti et al, 2007; De Angelis et al, 2012; Uggenti et al, 2014; Alessandrini et al, 2015), we focused our attention on the potential effects produced by M2 receptors in ADSCs. For this reason, the M2 receptor protein in ADSCs has been also confirmed by Western blot analysis (Fig.1C).

Positive autoregulation of M2 receptor subtype

Interistingly, we evaluated whether the M2 activation may induce an autocrine regulation of its expression on the ADSCs. To this aim, the ADSCs were treated with the M2 agonist APE (100μM). The M2 agonist treatment induces a higher expression of the M2 receptor transcript and protein as demonstrated by RT-PCR analysis and immunocytochemistry. This positive feedback was corroborated by the use of methoctramine, a preferential M2 antagonist. In fact the presence of M2 antagonist counteracted the up-regulated expression of M2 receptors induced by APE in ADSCs (Fig. 2A and 2B).

M2 receptor activation affects ADSCs proliferation

Thereafter, the ability of M2 muscarinic receptor to modulate ADSCs growth was evaluated by MTT assay. To this end, ADSCs were treated with M2 agonist APE that, as demonstrated in our previous studies by pharmacological competition experiments and M2 silencing (Ferretti et al, 2013; Alessandrini et al, 2015), is able to activate selectively only the M2 receptor. ADSCs were treated with 100μM APE for 24, 48 and 72h. As shown in Fig. 3A, the constrast phase light microscopy images indicated that ADSCs, in presence of APE, apparently decreased in cell number, compared to untreated cells. The MTT assay supported this observation, demonstrating that APE treatment significantly impaired ADSCs growth (Fig. 3B). In order to confirm that this effect was mediated by M2 receptors, the cells were treated with APE and M2 antagonist methoctramine (10^{-7}M). Moreover ADSCs were also treated with APE 100μM in co-presence of pirenzepine (10^{-7}M) and 4-DAMP (10^{-8}M), respectively M1 and M3 antagonists. The results obtained indicated that only methoctramine was able to counteract APE effects. In fact in presence of methoctramine, APE was not able to decrease ADSCs growth and the number of the cells appeared comparable to the untreated cells (Fig. 3B). Conversely, neither pirenzepine nor

4-DAMP were able to counterct APE effects (Fig. 3B). The analysis of cell viability indicated an apparently decrease of cell survival only after 24h of APE treatment, without any other significant change between treated and untreated cells at all time points considered; thus these results indicated that the decreased cell number observed after APE treatment was not dependent on APE toxicity (Fig. 3C).

In order to confirm the ability of M2 receptors to inhibit cell proliferation, cell cycle analysis on ADSCs maintained in the presence of 100μM APE for 48, 72 and 96 h, was performed. Before harvesting, cell cultures were pulsed with BrdU for 90 min to monitor S phase progression. The bi-parametric analysis of BrdU labelling versus DNA content, measured by propidium iodide, allowed the analysis of cell progression through the G1/S/G2 phases. As shown in Figure 4 and Table 2, the ADSCs showed a dramatic decrease in the BrdU labelled cell fraction after APE treatment. A decrease in the percentage of cells in the S phase after prolonged treatment was also observed with a progressive accumulation of the cells in the G1 phase.

The inhibition of cell proliferation was also confirmed by analysis of genes involved in cell proliferation. The analysis of PCNA and c-jun transcript levels demonstrated that APE treatment is able to significantly decrease their levels (Fig. 5A). The Western blot analysis for PCNA confirmed the decreased expression of the protein upon APE treatment, according to RT-PCR results (Fig. 5B). Similarly also cyclin D1 appeared significantly decreased after APE treatment, and the presence of methoctramine was able to re-establish the levels of cyclinD1 to the untreated cells (Fig. 5C). Considering the mitogenic effects of PDGF for MSCs (Rodrigues et al, 2010; Farahani et al, 2015), the basal expression of the PDGFR-β was also analysed in ADSCs. The RT-PCR analysis confirmed that ADSCs express PDGFR-β and that APE was able to significantly decreased its expression (Fig. 5A).

Finally, in order to establish whether the cell proliferation was recovered by M2 agonist withdrawl, ADSCs were treated with 100μM APE for 96h, then APE was removed and subsequently the cell number was assessed from 72 to 168h by MTT assay. After 96h in absence of M2 agonist, ADSCs were able to recover the proliferative state, although at lower levels if

compared to controls (Fig. 6A). The recovery of cell proliferation was accompained by the increased expression of genes involved in cell proliferation such as PDGFR-β and cyclinD1 (Fig.6B and 6C).

M2 receptors modulate ADSCs migration

To evaluate the M2 cholinergic agonist effect on cell migration, wound healing technique was performed (Fig.7A). When required from experimental plan, the muscarinic antagonists were added to the culture medium 2h before APE treatment. The migration was observed after 6h, in order to exclude the influence of cell proliferation, although the co-treatment with mitomycin C (an anti-tumor drug able to arrest cell proliferation) was also added. Six hours upon APE treatment, the distance of the gap between the two fronts was measured in the treated and untreated cells and compared respectively with their t0. The results indicated that the presence of M2 agonist APE impaired cell migration (Fig. 7A and 7B). The analysis of cell migration was also measured in presence of M2 antagonist, methoctramine and pirenzepine plus 4-DAMP, M1 and M3 antagonists respectively. After M1-M3 antagonists addition, ADSCs migration appeared comparable to APE treatment. Conversely, in presence of M2 antagonist methoctramine, the effect of APE was abolished and migration appeared comparable to untreated cells (Fig. 7A and 7B). The inhibitory effect of APE on cell migration was also confirmed by the Boyden's chamber assay; in fact the number of cells migrated in the below chamber, where the FBS was added as chemioattractant, was decreased in presence of 100μM APE compared with the untreated cells (Fig. 7C and 7D).

It is known that the CXCL12-CXCR4/CXCR7 axis is involved in migration and/or proliferation of several cells, including ADSCs (Li et al, 2013). By semiquantitave RT-PCR analysis, the CXCL12, CXCR4 and CXCR7 mRNA expression levels were analysed. After APE treatment, CXCR4 and CXCR7 expression were significantly reduced while CXCL12 expression appeared

not significantly affected (Fig. 8A). Similarly, Western blot analysis for CXCR4 and CXCR7 demonstrated a significant decrease of protein levels of the both receptors (Fig. 8B and 8C).

Discussion

Adipose tissue represents an attractive source of stem cells for regeneration, given their multipotentiality and ability to self-renewal. ADSCs can be obtained from various sources, but adipose tissue seems to be the most promising considering its availability, good accessibility and poor invasiveness in collecting. These cells have a great potential since can be amplified and differentiated *in vitro* in cells strains and transplanted to promote regeneration of several damaged tissues (Caddick et al, 2006; Kingham et al, 2007; Faroni et al, 2015).

ACh plays important roles in non-neural tissues, controlling proliferation, differentiation and migration in several cell types such as neural precursors cells, keratinocytes, lymphocytes and lung epithelial cells (Ma et al. 2000, Skok et al, 2006; Hoogduijn et al, 2009; Asrican et al 2016). However, no clear evidence on the role of ACh and its receptors in MSCs has bee reported. Our goal was to assess whether the ADSCs respond to ACh stimuli and which can be the effects produced. In this light, the ADSCs isolated from rat adipose tissue were used, confirming the stemness property through the analysis of specific markers. The colinoceptivity of these cells was then demonstrated by the analysis of the expression of different muscarinic receptor subtypes. Our interest was mainly focused on M2 receptors, that was proved to be mainly involved in the control of cell proliferation in several cell types (i.e. glial cells, neural precursors) (Ma et al, 2000; De Angelis et al, 2012; Loreti et al, 2007). In the ADSCs, M2 was activated by the selective agonist APE, a synthetic modified alkaloid derived by a metabolite produced by areca nut (Barlow et al, 1985). We previously demonstrated that APE was able to activate seletively only the M2 receptors (Loreti et al, 2007; De Angelis et al, 2012; Ferretti et al, 2013, Alessandrini et al, 2015). When ADSCs were treated with APE, cell growth as well as the expression of several genes involved in cell proliferation were significantly decreased. For

instance, c-jun, PCNA and cyclin D1 resulted decreased. Considering that cell viability was not affected by APE, M2 receptor activation was proposed as regulator of cell growth. In fact, the inhibition of cell proliferation was confirmed by flow cytometry analysis of ADSCs after BrdU incorporation. As indicated in table 2, the percentage of cells in S phase was strongly decreased upon M2 agonist treatment already at 48h of treatment and it remains substanstially unvariable at 72 and 96h. The decreased expression of PDGFR-β after APE treatment, suggested that the ability of M2 receptor to reduce cell proliferation may be dependent also on inhibition of PDGFR-β expression; this causes a decreased ability of ADSCs to respond to growth factors like PDGF-β (Rodrigues et al, 2010; Farahani et al, 2015). Interestingly the selective stimulation of M2 receptors appears related to a positive autocrine mechanism, that strength the M2-mediated outcomes observed in ADSCs.

The specific involvement of M2 was further evidenced by using the muscarinic antagonists. Indeed, pirenzepine and 4-DAMP, respectively antagonists of M1 and M3 receptor subtypes, or the use of methoctramine, specific M2 antagonist, showed that only the latter was able to conteract the APE effects, confirming that also in ADSCs, APE binds selectively the M2 muscarinic receptor. However, 96h after treatment and withdrawal of M2 agonist, ADSCs recover the cell proliferation, albeit maintaining a proliferative rate lower than the untreated cells. The proliferation rescue was also confirmed by increased gene expression of proliferation markers (i.e. PCNA, cyclin D1).

The migration is an other important MSCs characteristic. Here we demonstrate that M2 receptor activation was also able to inhibit ADSCs migration. In fact, in wound healing experiments, the APE-treated cells showed a decreased ability to migrate. Still using M1, M2 and M3 antagonists, it was observed that M2 agonist effects was counteracted only by methoctramine (M2 antagonist) thus demonstrating that M2 receptors negatively modulate ADSCs migration. Similarly, by the Boyden chamber assay, we demonstrated that the M2 receptor activation affects ADSC migration and the chemotactic ability of the cells to respond to the gradient of FBS, used as chemoattractant. In order to explain how M2 receptors impaired the ADSCs

migration, the ability of M2 receptors to modulate the expression of the CXCL12/SDF1-CXCR4/CXCR7 axis was also analysed. Both receptors are expressed in ADSCs, in particular after stimulation with SDF1. However, while CXCR4 appeared involved in the modulation of cell migration, the CXCR7 mediates the SDF-1 mitogenic effects on ADSCs (Li et al, 2013; Marquez and Wieczorek, 2013). In our experimental condition we demonstrated that APE negatively modulate the expression of CXCR4 and CXCR7 expression, both at mRNA and protein levels. The expression of SDF1-CXCL12, instead, was not modified by M2 agonist treatment. Our data suggest that M2 receptor activation negatively influence the effects mediated by SDF-1/CXCL12: preventing the chemokine' binding; in particular the decreasing of the CXCR4 expression may thus inhibit cell migration while the reduced expression of CXCR7, toghether with the reduced levels of PDGFR-β, may negatively influence the ADSCs proliferation.

In conclusion, our data demonstrate that ADSCs are cholinoceptive cells, responsive to M2 receptors selective activation. The activity of this receptor may contribute to maintain the stem cell pool in quiescent status, inhibiting, in reversible manner, the proliferative state and blocking cell migration. In agreement, these has been observed also for neural precursors in which, the M2 mediated mechanisms, control cell proliferation and differentiation (Ma et al, 2000). In these context, in particular for ADSCs, the modulated expression of PDGFR-β and CXCR7 receptors by M2 receptor activity may impair the action of growth factors such as PDGF-β and SDF-1/CXCL12, balancing the quiescent phase of ADSCs with the proliferative, migratory and differentiated phases. These findings may open new interesting perspectives on the control of ADSCs proliferation/differentiation overall for their use in regenerative medicine.

Conflict of Interest: The authors declare there are no conflicts of interest.

Acknowledgments: This work was supported by Ateneo Sapienza, University of Rome, Funds. RP fellowship was supported by Regione Lazio, Project "Torno subito 2015". The authors are grateful to Dr. Stefano Leone, University of Roma-3 for his helpul in Flow cytometry analysis and to Prof. Cristina Limatola that gently provided the CXCR4 and CXCR7 antibodies .

References

Alessandrini F, Cristofaro I, Di Bari M, Zasso J, Conti L, Tata AM. 2015. The activation of M2 muscarinic receptor inhibits cell growth and survival in human glioblastoma cancer stem cells. Int Immunopharmacol 29:105-109.

Asrican B, Paez-Gonzales P, Erb J, Kuo CT. 2016. Cholinergic circuit control postnatal neurogenesis. Neurogenesis 3: e1127310.

Barlow RB, Weston-Smith P. 1985. The relative potencies of some agonists at M2 muscarinic receptors in guinea pig ileum, atria and bronchi. Br J Pharmacol 85: 437–440.

Berger-Sweeney J, Hohmann CF. 1997. Behavioral consequences of abnormal cortical development: insights into developmental disabilities. Behav Brain Res 86: 121-142.

Bobis S, Jarocha D, Majka M. 2006. Mesenchymal stem cells: characteristics and clinical applications. Folia Histochem Cytobiol 44: 215-230.

Caddick J, Kingham PJ, Gardiner NJ, Wiberg M, Terenghi G. 2006. Phenotypic and functional characteristics of mesenchymal stem cells differentiated along a Schwann cell lineage. Glia 54: 840-849.

Chamberlain G, Fox J, Ashton B, Middleton J. 2007. Concise review: mesenchymal stem cells: their phenotype, differentiation capacity, immunological features, and potential for homing. Stem Cells 25: 2739-2749.

De Angelis F, Bernardo A, Magnaghi V, Minghetti L, Tata AM. 2012. Muscarinic receptor subtypes as potential targets to modulate oligodendrocyte progenitor survival, proliferation, and differentiation. Dev Neurobiol 72: 713-728.

Farahani RM, Xaymardan M 2015 Platelet-Derived Growth Factor Receptor Alpha as a Marker of Mesenchymal Stem Cells in Development and Stem Cell Biology. Stem Cells Int. e362753.

Faroni A, Mobasseri SA, Kingham PJ, Reid AJ. 2015. Peripheral nerve regeneration: experimental strategies and future perspectives. Adv Drug Deliv Rev. 82-83: 160-167.

Ferretti M, Fabbiano C, Di Bari M, Conte C, Castigli E, Sciaccaluga M, Ponti D, Ruggieri P, Raco A, Ricordy R, Calogero A, Tata AM. 2013. M2 receptor activation inhibits cell cycle progression and survival in human glioblastoma cells. J Cell Mol Med 17: 552-566.

Frith J, Genever P. 2008 Transcriptional control of mesenchymal stem cell differentiation. Transfus Med Hemother 35: 216-227.

Gimble JM, Katz AJ, Bunnell BA. 2007. Adipose-derived stem cells for regenerative medicine. Circ Res 11: 1249-1260.

Hoogduijn MJ, Cheng A, Genever PG. 2009. Functional nicotinic and muscarinic receptors on mesenchymal stem cells Stem Cells Dev. 18: 103-112.

Ilic D, Polak JM 2011 Stem cells in regenerative medicine: introduction. Br Med Bull 98: 117-126.

Karp JM., Leng Teo GS 2009. Mesenchymal Stem Cell Homing:The Devil Is in the Details. Cell Stem Cell, 4: 206-216.

Kingham PJ, Kalbermatten DF, Mahay D, Armstrong SJ, Wiberg M, Terenghi G. 2007. Adipose-derived stem cells differentiate into a Schwann cell phenotype and promote neurite outgrowth in vitro. Exp Neurol 207: 267-274.

Li Q, Zhang A, Tao C, Li X, Jin P. 2013. The role of SDF-1-CXCR4/CXCR7 axis in biological behaviors of adipose tissue-derived mesenchymal stem cells in vitro. Biochem Biophys Res Commun 441: 675-680.

Loreti S., Ricordy R., De Stefano ME., Augusti-Tocco G., Tata AM., 2007. Acetylcholine inhibits cell cycle progression in rat Schwann cell by activation of the M2 receptor subtype. Neuron Glia Biol 3: 269-279.

Loreti S., Vilarò M.T., Visentin S., Rees H., Levey A.I, Tata A.M. 2006. Rat Schwann cells express M1-M4 muscarinic receptor subtypes. J Neurosci Res 84: 97-105.

Ma W, Maric D, Li BS, Hu Q, Andreadis JD, Grant GM, Liu QY, Shaffer KM, Chang YH, Zhang L, Pancrazio JJ, Pant HC, Stenger DA, Barker JL. 2000. Acetylcholine stimulates cortical precursor cell proliferation in vitro via muscarinic receptor activation and MAP kinase phosphorylation. Eur J Neurosci 12: 1227-1240.

Morris D. 1966. The choline acetyltransferase of human placenta. Biochem J. 98: 754-762.

Patel DM, Shah J, Srivastava AS. 2013. Therapeutic potential of mesenchymal stem cells in regenerative medicine. Stem Cells Int: e496218.

Rodrigues M, Griffith LG, Wells A. 2010. Growth factor regulation of proliferation and survival of multipotential stromal cells. Stem Cell Res Ther 1: 32.

Ryu YJ, Cho TJ, Lee DS, Choi JY, Cho J. 2013. Phenotypic characterization and in vivo localization of human adipose-derived mesenchymal stem cells. Mol Cells 35: 557-564.

Skok M, Grailhe R, Agenes F, Changeux JP. 2006. The role of nicotinic acetylcholine receptors in lymphocyte development. J Neuroimmunol 171: 86-98.

Strem BM, Hicok KC, Zhu M, Wulur I, Alfonso Z, Schreiber RE, Fraser JK, Hedrick MH. 2005. Multipotential differentiation of adipose tissue-derived stem cells. Keio J Med 54:132-141.

Uggenti C, Costantino M., Pisano A., De Stefano M.E., Magnaghi V., Talora C., Wess J., Tata A.M. 2014. M2 muscarinic receptors activation contributes to modulate Schwann cell migration and differantiation in mielinating phenothype. Dev Neurobiol. 74: 676-691.

Vindigni V., Giatsidis G., Reho F., Dalla Venezia E., Mammana M. Bassetto F. 2013. Adipose derived stem cells: current state of the art and the prospective role in regenerative medicine and tissue engineering. Reg Med and Tissue Eng. Chap. 8 edit. by Jose A. Andrades, ISBN 978-953-51-1108-5.

Weissman IL. 2000. Stem cells: units of development, units of regeneration, and units in evolution. Cell 100: 157–168.

Wessler I, CJ Kirkpatrick and K Racke. 1999. The cholinergic "pitfall": acetylcholine, a universal cell molecule in biological systems, including humans. Clin Exp Pharmacol Physiol 26: 198–205.

Figure Legends

Figure 1. Stemness markers and muscarinic receptor subtypes expression.

A) Stemness marker expression was assessed by RT-PCR. Fibroblasts was used as control of differentiated cells. B) RT-PCR analysis shows ADSCs expressing all muscarinic receptors, except M5. In particular M2 and M3 expression appears more prominent. GAPDH was used as housekeeping gene. C) Western Blot shows M2 muscarinic receptors expression; rat brain was used as positive control. β-actin was used as protein reference.

Figure 2. Positive feedback of M2 receptor expression.

A) RT-PCR analysis of M2 receptors in ADSCs in absence or presence of M2 agonist (APE). M2 antagonist methoctramine (Meth) was used to conteract the APE effects. The graphs show the densitometric analysis of the band normalized for the housekeeping GAPDH. The results are the media ± SEM obtained from three independent experiments. B) Immunocytochemistry analysis for M2 receptor in ADSCs in absence or presence of APE and APE plus methoctramine (200x).

Figure 3. The activation of M2 receptors causes an inhibition of cell growth

A) ADSCs cultures shows a flattened *fibroblast-like* morphology. Cells treated with APE appears at lower density compared to untreated cells (100x). B) Analysis of cell growth by MTT assay upon100μM APE treatment. M2 agonist causes a decreased cell growth in time dependent manner. The cell proliferation has been also evaluated in cultures maintained in the presence of 100μM APE plus M1 and M3 antagonists (10^{-7}M Pirenzepine; (Pire), 10^{-8}M 4-DAMP, respectively) and 100μM APE plus M2 antagonists (10^{-7}M Methoctramine; Meth). The presence of the M1 and M3 antagonists does not counteract the M2 agonist effects, demonstrating that these receptors are not involved in the APE inhibition of the cell growth. Instead, Meth, a preferring M2 antagonist, is able to counteract the APE effects. C) APE treatment does not

influence cell viability. The results are the media ± SEM of three independent experiments performed in triplicate. (* $p<0.05$; ** $p< 0.01$; ***$p<0.001$).

Figure 4. Flow cytometry analysis of ADSCs after BrdU incorporation.

Bivariate analysis of BrdU incorporation (ordinate) and DNA content (abscissa) in ADSCs at 48, 72, 96h in untreated (ctrl) and 100μM APE treated cells. The BrdU labelled cell fraction appears dramatically reduced after APE treatment (S phase) (pink area).

Figure 5. The selective activation of M2 receptors causes an inhibition of cell proliferation markers

A) RT-PCR expression analysis of cell proliferation markers in ADSCs upon 100μM APE. According to MTT analysis, APE treatment causes a significant decrease of cyclinD1, PCNA, c-jun, PDGFR-β trascripts. The graphs indicated the densitometric analysis of the bands obtained in three independent experiments, normalized for GAPDH gene. B) Western Blot and densitometric analysis of PCNA protein levels in untreated (ctrl) and 100μM APE treated cells (24 and 48h). β-actin was used as protein reference. (N=3; *$p<0.05$). C) M2 receptors activation induces an inhibition of cyclinD1 transcript, while the presence of M2 antagonist, Meth, counteracts the APE effects, determining a cyclinD1 expression comparable to control. The graph indicates the densitometric analysis of the bands obtained in three independent experiments and normalized for GAPDH gene expression, used as housekeeping genes.

Figure 6. Recovery assay

A) ADSCs proliferation was assessed after 96h in absence and in presence of APE (100μM), then APE was removed and the cell growth was analysed from 72 until 168h by MTT assay. After 96h ADSCs were able to recover the cell proliferation although maintaining a lower proliferative rate than control. B) The rescue of cell proliferation was confirmed by the analysis of c-jun, pcna, cyclinD1 and PDGFR-β transcripts. All mRNA levels appear increased after APE

removing from the cell culture. C) the graphs indicate the densitometric analysis of the RT-PCR analysis. The GAPDH was used as housekeeping gene. The results are the media ± SEM of three independent experiments performed in triplicate. (* $p<0.05$; ** $p< 0.01$; ***$p<0.001$).

Figure 7. Analysis of cell migration

A) The analysis of cell migration was performed by wound healing assay. The images have been obtained at time 0 (t0) corresponding to time in which the scratch has been performed, and after 6h (t6), to analyse the width of scratch in absence or presence of M2 agonist and antagonists (50x). B) the graph indicates the size of the scratch at all the experimental conditions. C) Boyden Chamber'assay: Microscopic images of ADSCs cultures, exposed to 100µM APE, in which the migrated cells were stained in purple (150x). D) 24h exposure of ADSCs to 100µM APE decreased significantly (**$p<0.01$) the migration versus a chemotactic agent FBS 1%. Migrating cell number (per area in squared mm) of ADSC exposed (grey column) was calculated and compared with the controls (Ctrl, white column). The values are means ± SEM. (N=9). (** $p< 0.01$; ***$p<0.001$).

Figure 8. Analysis of CXCL12-CXCR4/CXCR7 axis

A) RT-PCR analysis of CXCL12, CXCR4 and CXCR7 expression after 100µM APE treatment. The graphs below indicate the densitometric analysis of the bands normalized with GAPDH, used as housekeeping gene. The results are the media ± SEM of three independent experiments. (* $p<0.05$; ** $p< 0.01$; ***$p<0.001$). B) Western Blot and densitometric analysis for CXCR4 protein in untreated (ctrl) and APE (100µM) treated cells (24 and 48 h). β-actin was used as protein reference (N=3) (*$p< 0.05$; **$p<0.01$). C) Western Blot and densitometric analysis for CXCR7 protein in untreated (ctrl) and APE (100µM) treated cells (24 and 48 h). β-actin was used as protein reference (N=3) (*$p< 0.05$; **$p<0.01$).

Table 1. *Primers sequences used in semiquantitative RT-PCR analysis*

Primers sequences (RT-PCR)	**Forward**	**Reverse**
M1	5'-CCATGGAGTCCCTCACATCCT-3'	5'-ATCTACCATGGGCATCTTGATCA-3'
M2	5'-GCTCCAATGATTCGACGTCA-3'	5'-CGAAGTGGAAACTGTTGTTTTCAT-3'
M3	5'-TCCATCCTCAACTCTACCAAGCT-3'	5'-TTGTGAGCATTTCTCTCCACATC-3'
M4	5'-CACTCTGCAATGCCACTTTCAA-3'	5'-CTGTGCCGATGTTCCGATACT-3'
M5	5'-ACCCGCACTGAAAACAGTGACT-3'	5'-ATCGGAACTAGGCAACACACTT-3'
cyclinD1	5'-CCCTCTGCACGCACTTGAAG-3'	5'-GCGAGCCATGCTTAAGACTGA-3'
pcna	5'-GAAGCACCAAATCAAGAGAA-3'	5'-TCACCCCGTCCTTTGCACAG-3'
CD29	5'-TGGGTCGCTGATTGGCTG-3'	5'-CTCTTCAGTGACTGCAAAAATCG-3'
CD44	5'-TCATGTTAGAGCATCCGTGC-3'	5'-GGGTTGTACATCATGCCTCC-3'
CD90	5'-TGAACCCAGTCATCAGCAT-3'	5'-CAGTCGAAGGTTCTGGTTCACC-3'
c-jun	5'-GATGGAAACGACCTTCTACGAC-3'	5'-AGCGTATTCTGGCTATGCAGTT-3'
CXCL-12	5'-TGCATCAGTGACGGTAAGCCA-3'	5'-ATCCACTTTAATTTCGGGTCAA-3'
CXCR-4	5'-GCCATGGCTGACTGGTACTT-3'	5'-GATGAAGGCCAGGATGAGAA-3'
CXCR-7	5'-GGCTACGACACACACTGCTA-3'	5'-GGTCCACGCTCATGCATGCG-3'
Pdgfr-β	5'-CAACATTTCGAGCACCTTTGT-3'	5'-AGGGCACTCCGAAGAGGTAA-3'
gapdh	5'-GTGCCAGCCTCGTCTCATAG-3'	5'-TGATGGCAACAATGTCCACT-3'

Table 2. *Percentage of cells in G1, S, G2/M phases after 100 μM APE treatment. The data are the mean ±SEM. P values are also reported (APE treated cells vs ctrl)*

	G1 (%)	SEM	P	S (%)	SEM	P	G2/M	SEM
Ctrl 48h	80,05	2		9,29	0,7		9,76	2
APE 48h	91,3	2,1	0,05	0,71	0,1	0,001	7,36	2,36
Ctrl 72h	75,05	0,3		10,27	0,1		9,32	3,5
APE 72h	88,9	0,1	0,01	0,8	1,5	0,001	6,5	3,1
Ctrl 96h	75,59	4		6,115	1,4		10,06	3,1
APE 96h	92,045	1,1	0,001	0,67	0,1	0,001	5,85	2,1

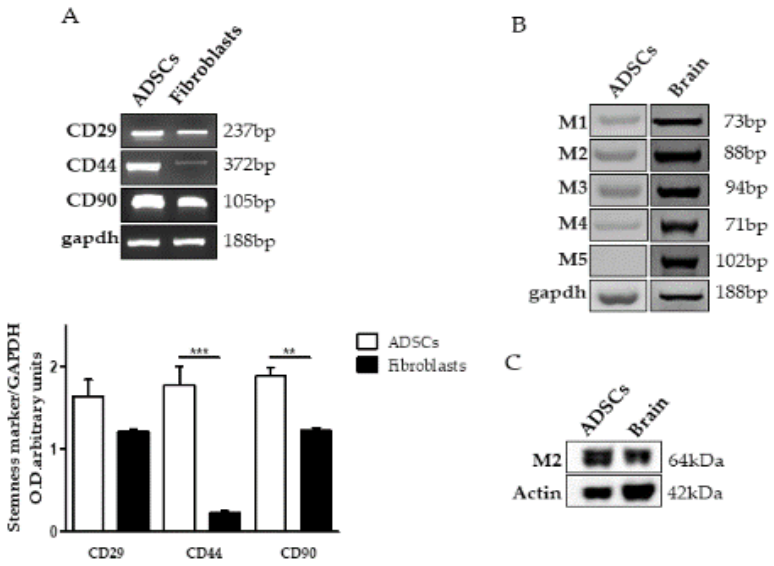

Figure 1

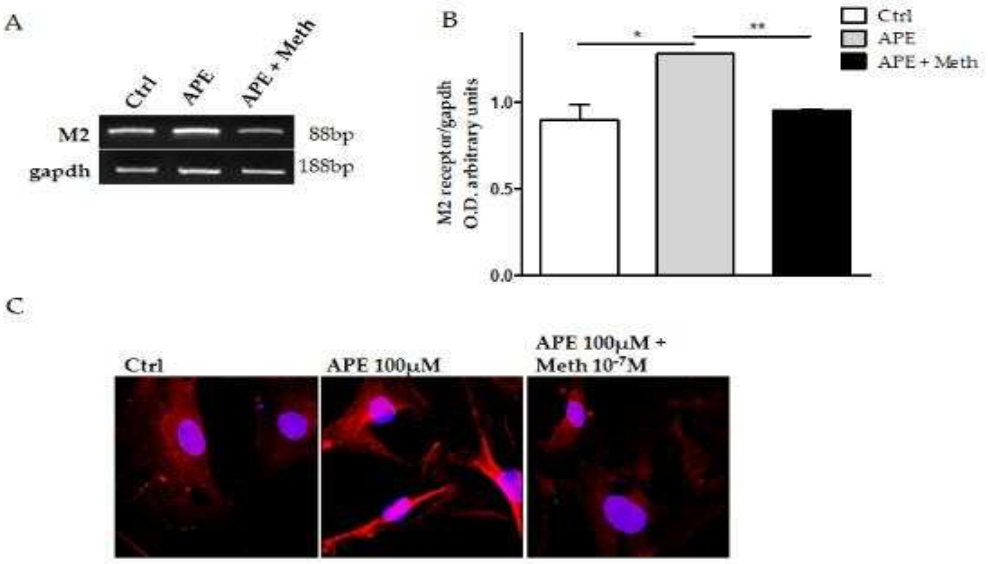

Figure 2

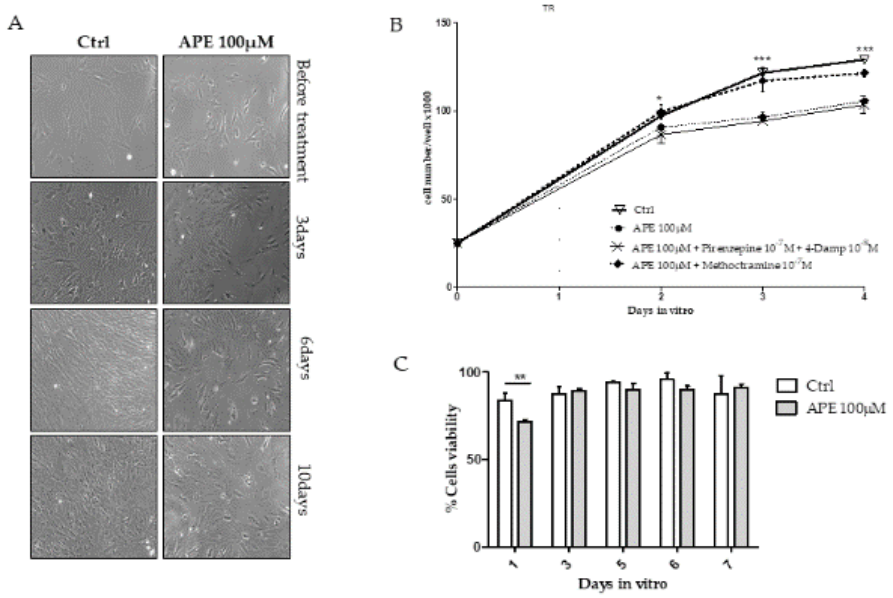

Figure 3

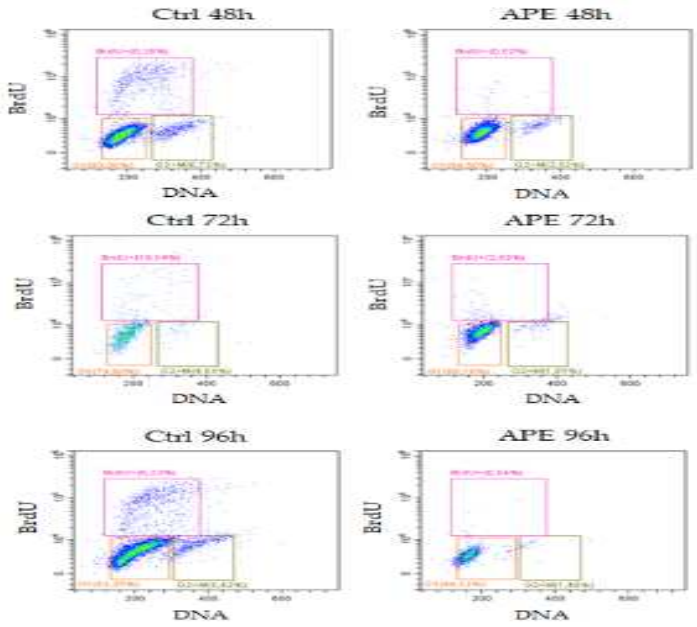

Figure 4

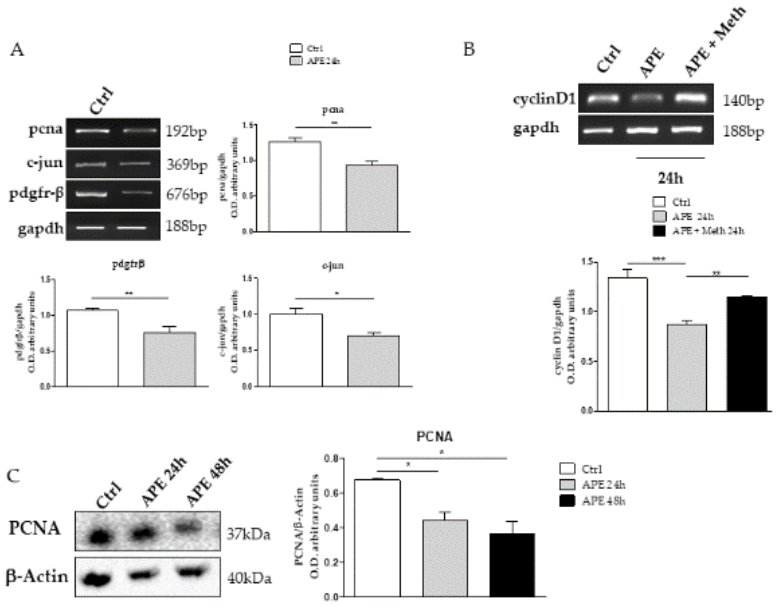

Figure 5

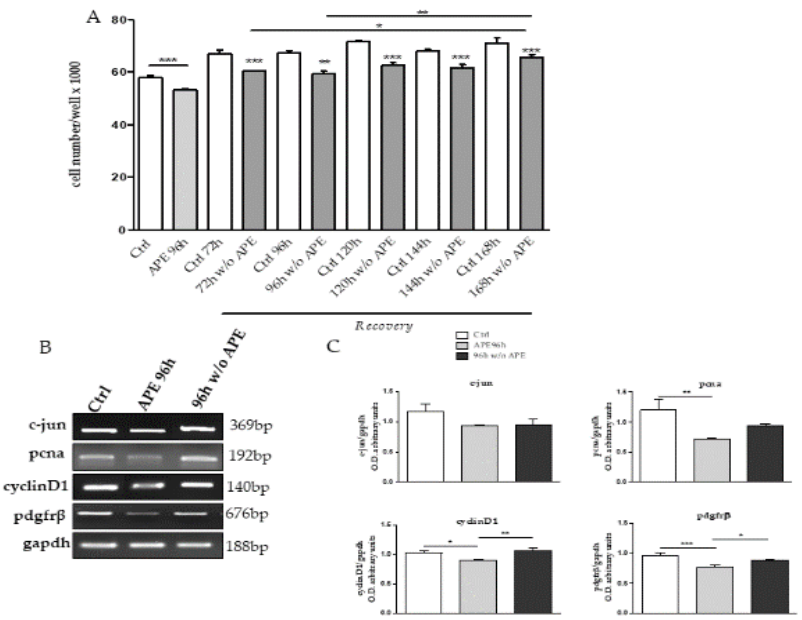

Figure 6

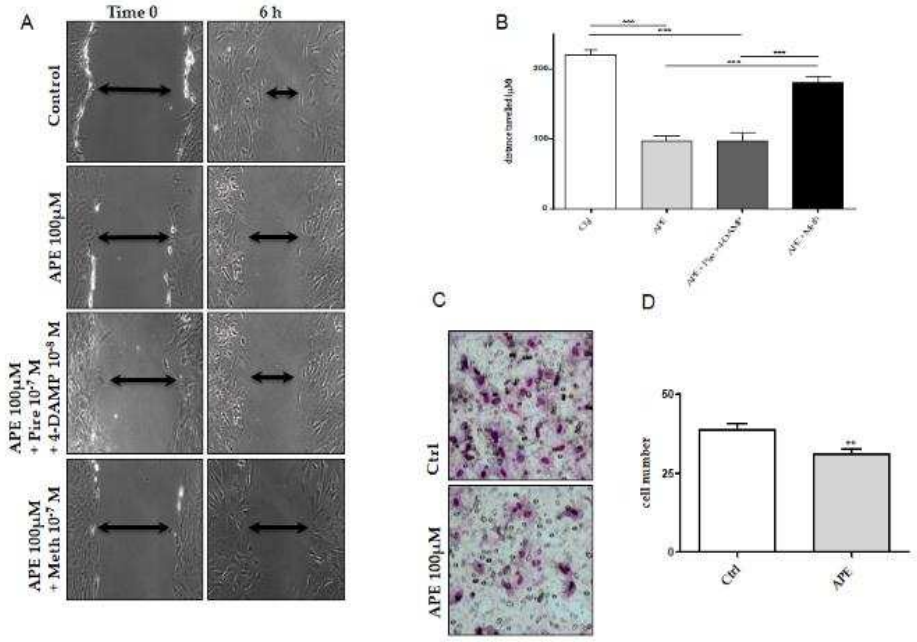

Figure 7

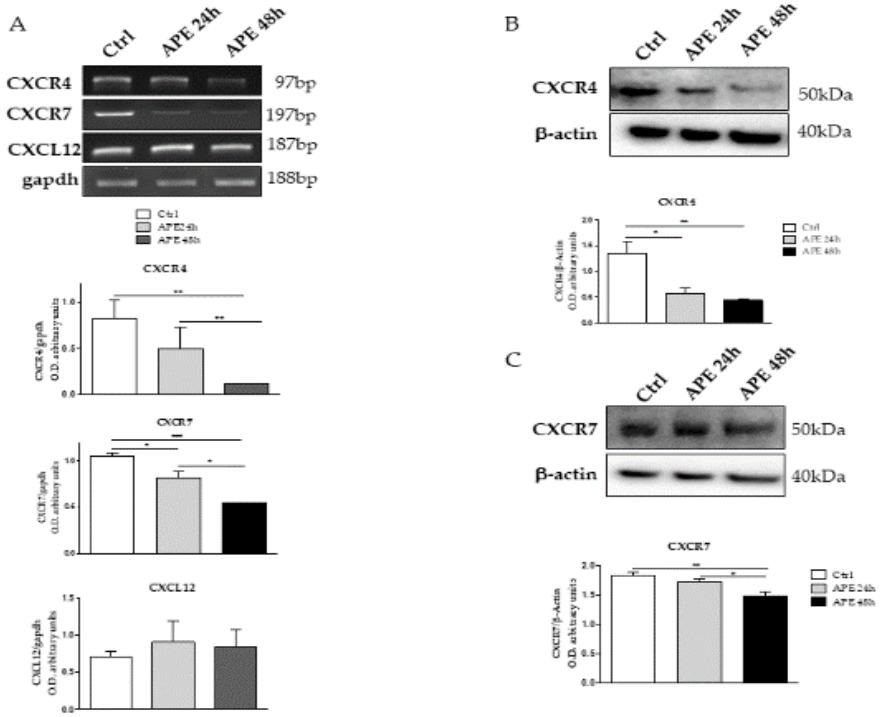

Figure 8